

# Testing for multifractality of the slow solar wind

Wiesław M. Macek<sup>a,b,\*</sup>, Roberto Bruno<sup>c</sup>, Giuseppe Consolini<sup>c</sup>

<sup>a</sup> Faculty of Mathematics and Natural Sciences, College of Sciences, Cardinal Stefan Wyszyński University, Dewajtis 5, 01-815 Warsaw, Poland

<sup>b</sup> Space Research Centre, Polish Academy of Sciences, Bartycka 18 A, 00-716 Warsaw, Poland

<sup>c</sup> Istituto di Fisica dello Spazio Interplanetario, Istituto Nazionale di Astrofisica, Via Fosso del Cavaliere 100, 00-133 Roma, Italy

Received 28 October 2004; received in revised form 11 February 2005; accepted 28 June 2005

## Abstract

We analyse a time series of the radial component of the Elsässer variable for the low-speed stream of the solar wind plasma representing Alfvénic fluctuations propagating downstream as measured in situ by the Helios spacecraft in the inner heliosphere. We demonstrate that the influence of noise in the data can be efficiently reduced by moving average and singular-value decomposition filters. We calculate the multifractal spectrum for the flow of the solar wind directly from the cleaned experimental signal. The resulting spectrum of dimensions shows a multifractal structure of the solar wind in the inner heliosphere. The obtained multifractal spectrum is consistent with that for the multifractal measure on the self-similar weighted Cantor set with the degree of multifractality of  $\sim 10^{-1}$ .

© 2006 Published by Elsevier Ltd on behalf of COSPAR.

**Keywords:** Time series analysis; Solar wind plasma; Fractals; Chaotic dynamics

## 1. Introduction

The generalized dimensions of attractors are important characteristics of complex dynamical systems. Since these dimensions are related to frequencies with which typical orbits in phase space visit different regions of the attractors, they provide information about dynamics of the systems (Grassberger, 1983; Hentschel and Procaccia, 1983; Halsey et al., 1986; Ott, 1993). If the measure has different fractal dimensions on different parts of the support, the measure is multifractal (Mandelbrot, 1989).

The question of multifractality is of great importance also for the solar wind community, because it allows to investigate the nature of interplanetary hydromagnetic

turbulence (e.g., Marsch and Tu, 1997; Burlaga, 2001; Bruno et al., 2001). As a matter of fact multifractality is related to intermittency (e.g., Carbone, 1993; Carbone and Bruno, 1996). In particular, the multifractal spectrum was investigated with Voyager (magnetic field) data in the outer heliosphere (e.g., Burlaga, 1991) and with Helios (plasma) data in the inner heliosphere (e.g., Marsch et al., 1996). Therefore, following other space physics applications (e.g., Kurths and Herzog, 1987), we consider the inner heliosphere. The solar wind plasma flowing supersonically outward from the Sun is quite well modelled within the framework of the hydromagnetic theory. It is well known, based on, e.g., Helios experimental data, that the velocity of the solar wind varies widely, in general between about  $300 \text{ km s}^{-1}$  (slow solar wind streams) and about  $900 \text{ km s}^{-1}$  (fast solar wind streams) Schwenn (1990). The fast wind is associated with coronal holes and is relatively uniform and stable, while the slow wind is quite variable in terms of velocities. We limit our study to the low-speed stream.

\* Corresponding author. Tel.: +4822 840 3766x309; fax: +4822 840 3131.

E-mail address: [macek@cbk.waw.pl](mailto:macek@cbk.waw.pl) (W.M. Macek).

URL: <http://www.cbk.waw.pl/~macek> (W.M. Macek).

Indication for a chaotic attractor in the slow solar wind has been given by Macek (1998), Macek and Obojska (1997), Macek and Obojska (1998), Macek and Redaelli (2000), Macek (2002). In particular, Macek (1998) has calculated the correlation dimension of the reconstructed attractor and has provided tests for *nonlinearity* in the solar wind data, including a powerful method of singular-value decomposition (Albano et al., 1988) and statistical surrogate data tests (Theiler et al., 1992). Further, Macek and Redaelli (2000) have shown that the Kolmogorov entropy of the attractor is *positive* and finite, as it holds for a *chaotic* system. The entropy is plausibly constrained by a *positive* local Lyapunov exponent that would exhibit sensitive dependence on initial conditions of the system.

Recently, we have extended our previous results on the dimensional time series analysis (Macek, 1998). Namely, we have applied the technique that allows a realistic calculation of the generalized dimensions of the solar wind flow directly from the cleaned experimental signal by using the Grassberger and Procaccia (1983) method. The resulting spectrum of dimensions shows the multifractal structure of the solar wind in the inner heliosphere (Macek, 2002). The obtained multifractal spectrum is consistent with that for the multifractal measure on the self-similar weighted Cantor set. In this paper we demonstrate the influence of noise on these results and show that noise can efficiently be reduced by a singular-value decomposition filter, which is sufficient to calculate the generalized dimensions of the solar wind attractor. The obtained value of the degree of multifractality is discussed in the context of the  $p$ -model of turbulence cascade (e.g., Meneveau and Sreenivasan, 1987).

## 2. Data

We analyse the Helios 2 data using plasma parameters measured in situ in the inner heliosphere (Schwenn, 1990). The radial velocity component of the plasma flow,  $v$ , has been investigated by Macek (1998) and Macek and Redaelli (2000). However, it is known that various disturbances are superimposed on the overall structure of the solar wind, including mainly Alfvén waves, which move away from the Sun. Therefore, in this paper we take also into account Alfvénic fluctuations of the flow. Namely, in this paper we analyse the radial component of one of the Elsässer variables,  $x = z_+$ , representing Alfvénic fluctuations propagating radially outward from the Sun. We have  $z_+ = v + v_A$  for the unperturbed magnetic field  $B_0$  pointing to the Sun and  $z_+ = v - v_A$  for  $B_0$  pointing away from the Sun, where  $v_A = B/(\mu_0\rho)^{1/2}$  is the Alfvénic velocity calculated from the experimental data: the radial component of the magnetic field of the plasma  $B$  and the mass density  $\rho$  ( $\mu_0$  is the permeability of free space).

We have selected a time interval observed by the Helios 2 spacecraft in 1977 from 116:00 to 121:21 (day:hour) at distances 0.30–0.34 AU from the Sun. These raw data of  $v$  and  $v_A$ ,  $N = 10,644$  points, with sampling time of  $\Delta t = 40.5$  s, are shown in Fig. 1 (a).

As in Macek (2002), slow trends  $342.534 - 0.0495t - 0.0007t^2$ , and  $84.31 - 3.175t + 0.01736t^2$  (with  $t$  being a time of a sample in hours) were subtracted from the original data  $v(t_i)$ , and  $v_A(t_i)$ , correspondingly, where these values are given in  $\text{km s}^{-1}$ , and  $i = 1, \dots, N$ . The data with the initial several-percent noise level were (eight-fold) smoothed (replacing each data point with the average of itself and its two nearest neighbours). Next, the data have been filtered using a powerful method of singular system (singular-value decomposition or principal component) analysis described by Albano et al. (1988). Basically, noise prevents any eigenvalue or principal

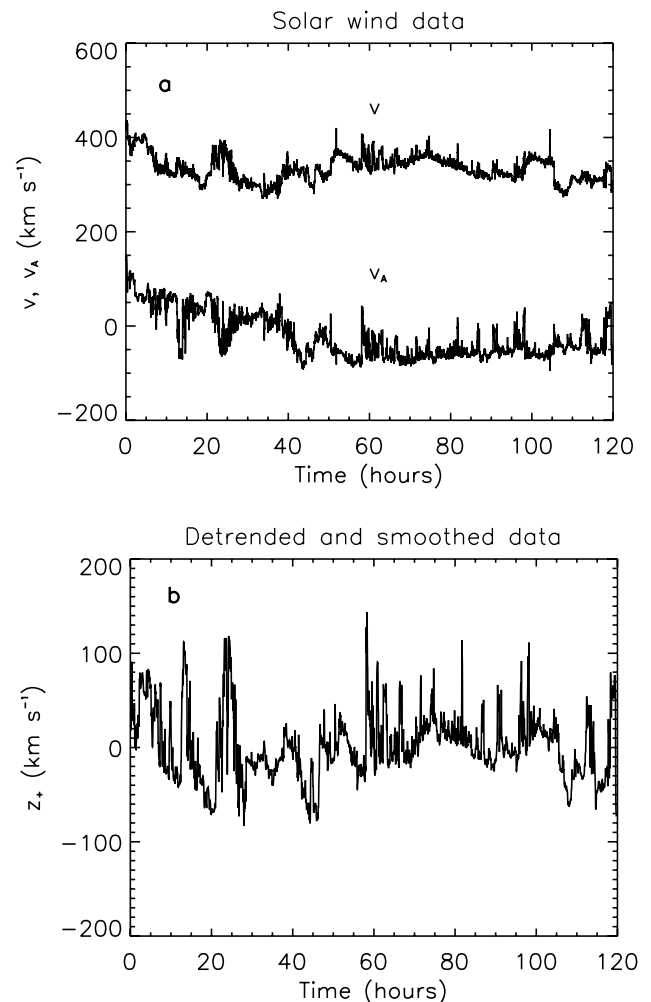


Fig. 1. (a) The raw data of the radial flow velocity with Alfvénic velocity,  $v$  and  $v_A$ , observed by the Helios 2 spacecraft in 1977 from 116:00 to 121:21 (day:hour) at distance 0.3 AU from the Sun, (b) the radial component of the Elsässer variable  $z_+ = v \pm v_A$  for  $B_0$  pointing to/away from the Sun for the detrended and filtered data using singular-value decomposition with the five largest eigenvalues.

component from vanishing. Hence by limiting the number of basic eigenvectors, by taking only those corresponding to some large eigenvalues, a substantial amount of the inherent noise of the experimental data is removed. As argued by Macek (1998) we use five principal eigenvalues. The detrended and filtered data for the radial component of the Elsässer variable  $z_+$  are shown in Fig. 1(b). Certainly, this linear filtering removes considerable amount of noise, leaving only few percents. The nonlinear filtering, which allows calculation of the entropy, has been discussed by Macek and Redaelli (2000). It has been shown that after the nonlinear Schreiber filter the calculated dimension has been somewhat reduced. In this paper, we focus on the calculations of dimensions. Therefore, we use moving average and singular-value decomposition filtering (cf. Macek, 1998).

Table 1 summarizes selected calculated characteristics of the detrended data cleaned by using the singular-value decomposition filter, see also (Macek, 2002). The probability distributions are clearly non-Gaussian (cf. Marsch and Tu, 1994). We have a large skewness of  $\sim 0.57$  (as compared with its normal standard deviation 0.04) and a large kurtosis of 0.66 (the latter was small for the analysis with no magnetic field) (cf. Macek, 1998). We have also estimated the Lempel–Ziv measure of *complexity*, relative to white noise (Kaspar and Schuster, 1987). The calculated value  $\sim 0.11$  is even smaller than in (Macek, 1998) ( $\approx 0.20$ ); maximal complexity, or randomness, would have a value of 1.0, while a value of zero denotes perfect deterministic nonlinear predictability.

For a given time series the values are normalized to the unit interval, dividing by the maximal value. As shown in Fig. 2 the normalized autocorrelation function for detrended and filtered data displays important oscillations that reveal aperiodic behaviour of the flow of the solar wind. In particular, the autocorrelation first falls steeply to a value of  $1 - 1/e$  in less than half an hour ( $36\Delta t$ ) then decreases nearly linearly, reaching a value of  $1/2$  at  $3/4$  h, and a value of  $1/e$  at the autocorrelation time  $t_a = 122\Delta t = 1.37$  h,  $(\langle x(t)x(t+t_a) \rangle - \langle x(t) \rangle^2) / \sigma^2 = 1/e$ , with average velocity  $\langle x \rangle = 1.528$  km s $^{-1}$  and standard deviation  $\sigma = 35.33$  km s $^{-1}$ , (cf. Macek, 1998, Fig. 2 (b)) (see also Table 1). Obviously, for an ideally periodic system the optimum time delay for attractor

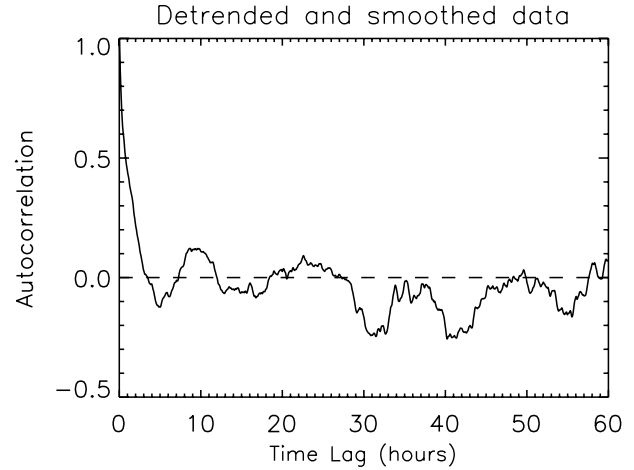


Fig. 2. The normalized autocorrelation function as a function of the time lag for the detrended and filtered data.

reconstruction would be one-quarter of the natural orbital period, i. e., the first zero of the autocorrelation function. The value of the autocorrelation time is only somewhat smaller than  $t_0 = 310\Delta t = 3.5$  h, the first actual zero of the autocorrelation function. Therefore, for our aperiodic system we choose a time delay equal to the autocorrelation time  $t_a$ , i.e.,  $\tau = 122\Delta t$ . This makes certain that  $x(t)$  and  $x(t + \tau)$  are at least linearly time independent (e.g., Ott, 1993).

### 3. Generalized dimensions

Using our time series of equally spaced, detrended and cleaned data, we construct a large number of vectors  $\mathbf{X}(t_i) = [x(t_i), x(t_i + \tau), \dots, x(t_i + (m - 1)\tau)]$  in the embedding phase space of dimension  $m$ , where  $i = 1, \dots, n$  with  $n = N - (m - 1)\tau$ . Then, we divide this space into a large number  $M(r)$  of equal hypercubes of size  $r$  which cover the presumed attractor, where  $r$  is distance between normalized vectors. If  $p_j$  is the probability measure that a point from a time series falls in a typical  $j$ th hypercube, using the  $q$ -order function  $I_q(r) = \sum (p_j)^q$ ,  $j = 1, \dots, M$ , the  $q$ -order generalized dimension is given by Hentschel and Procaccia (1983), Halsey et al. (1986) and Ott (1993)

$$D_q = \frac{1}{q-1} \lim_{r \rightarrow 0} \frac{\ln I_q(r)}{\ln r}. \quad (1)$$

We see from Eq. (1) that the larger  $q$  is, the more strongly are the higher probability cubes (visited more frequently by a trajectory) weighted in the sum for  $I_q(r)$ . Intuitively, the generalized dimensions quantify multifractality. Namely, if different parts of the phase space of the dynamical system are visited with different probability, then  $D_q$  is a nonconstant function of  $q$ . Only if  $q = 0$ , all the cubes are counted equally,  $I_0 = M$ , and we recover the box-counting dimension,  $D_0$ .

Table 1  
Characteristics of the solar wind filtered data,  $z_+$

Skewness, $\kappa_3$	0.57
Kurtosis, $\kappa_4$	0.66
Relative complexity	0.11
Autocorrelation time, $t_a$	$4.9 \times 10^3$ s
Capacity dimension, $D_0$	3.5
Correlation dimension, $D_2^a$	3.1

<sup>a</sup> The average slope for  $6 \leq m \leq 10$  is taken as  $D_q$ .

Writing  $I_q(r) = \sum p_j(p_j)^{q-1}$  as a weighted average  $\langle (p_j)^{q-1} \rangle$ , one can associate bulk with the generalized average probability per hypercube  $\mu = \sqrt[q-1]{\langle (p_j)^{q-1} \rangle}$ , and identify  $D_q$  as a scaling of bulk with size,  $\mu \propto r^{D_q}$ . Since the data cannot constrain well the capacity dimension  $D_0$ , we look for higher-order dimensions, which quantify the multifractality of the probability measure on the attractor. For example, the limit  $q \rightarrow 1$  leads to a geometrical average (the information dimension). For  $q = 2$  the generalized average is the ordinary arithmetic average (the standard correlation dimension), and for  $q = 3$  it is a root-mean-square average. In practice, for a given  $m$  and  $r$ ,

$$p_j \simeq \frac{1}{n - 2n_c - 1} \sum_{i=n_c+1}^n \theta(r - |\mathbf{X}(t_i) - \mathbf{X}(t_j)|) \quad (2)$$

with  $\theta(x)$  being the unit step function, and  $n_c = 2$  is the Theiler's (1986) correction. Finally,  $I_q(r)$  is taken to be equal to the generalized  $q$ -point correlation sum (Grassberger and Procaccia, 1983)

$$C_q(m, r) = \frac{1}{n_{\text{ref}}} \sum_{j=1}^{n_{\text{ref}}} (p_j)^{q-1}, \quad (3)$$

where  $n_{\text{ref}} = 5000$  is the number of reference vectors. For large dimensions  $m$  and small distances  $r$  in the scaling region it can be argued that  $C_q(m, r) \propto r^{(q-1)D_q}$ , where  $D_q$  is an approximation of the ideal limit  $r \rightarrow 0$  in Eq. (1) for a given  $q$  (Grassberger and Procaccia, 1983).

#### 4. Results and discussion

First, we calculate the natural logarithm of the standard ( $q = 2$ ) correlation sum  $C_m(r) = C_2(m, r)$  versus  $\ln r$  (normalized) for various embedding dimensions:  $m = 4$  (dotted curve),  $m = 5$  (diamonds),  $m = 6$  (triangles),  $m = 7$  (squares),  $m = 8$  (crosses),  $m = 9$  (pulses), and  $m = 10$  (stars) signs. The slopes  $D_{2,m}(r) = d[\ln C_m(r)]/d(\ln r)$  in the scaling region of  $r$  should provide the correlated dimension. The results obtained using the moving average and singular-value decomposition linear filters are presented in Fig. 3, while those obtained using the nonlinear Schreiber filters have been discussed by Macek (1998) and Macek and Redaelli (2000). Since the correlation sum is simply an arithmetic average over the numbers of neighbours, this can yield meaningful results for the dimension even when the number of neighbours available for some reference points is limited in most real dynamical systems. If the  $D$ -dimensional attractor exists, we expect a plateau of the slopes for  $m \geq D$  and in the worst case for  $m > 2D$ . For  $m$  large enough an average slope in the scaling region indicates a proper correlation slope dimension  $D_2$ . We have a clear plateau which appears already for  $m = 4$  (dotted curve) and  $m = 5$ . For higher dimensions,  $m \geq 8$ , the plateau is still

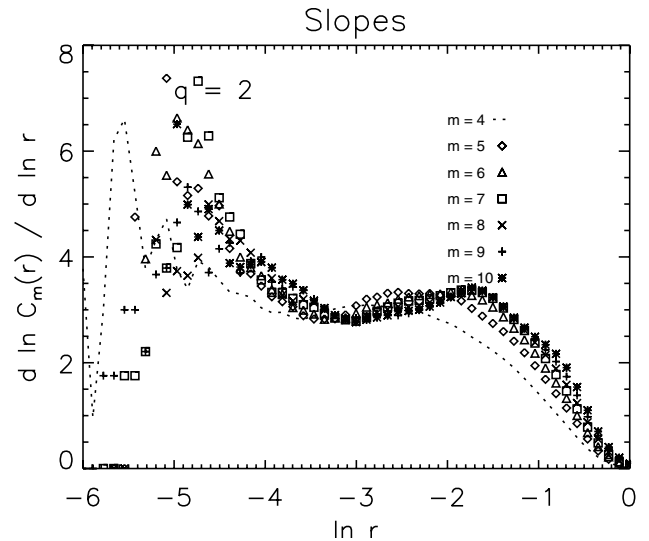


Fig. 3. The slopes  $D_{2,m}(r) = d[\ln C_m(r)]/d(\ln r)$  of the correlation sum  $C_m(r)$  versus  $\ln r$  (normalized) obtained for detrended and filtered data are shown for various embedding dimensions  $m$ .

present but more smeared out by the statistical fluctuations at small  $r$ . In our case of the singular-value decomposition filter the slope of the calculated correlation sum saturates for  $m > 5$ , with an average for  $6 \leq m \leq 10$  of  $D_2 = 3.13 \pm 0.07$  (cf. Macek, 1998); this is consistent with the attractor of the low-dimension.

Second, the generalized dimensions  $D_q$  in Eq. (1) as a function of  $q$  are shown in Fig. 4. In spite of large statistical errors the multifractal character of the measure can still be discerned. Therefore, one can say that the spectrum of dimensions shows the multifractal structure of

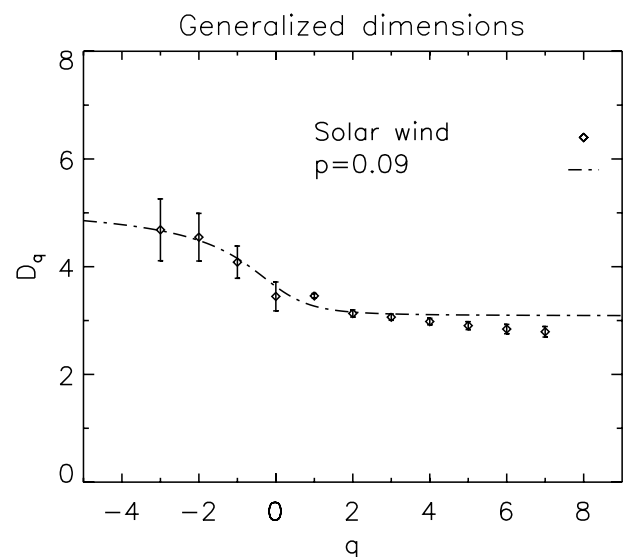


Fig. 4. The generalized dimensions  $D_q$  in Eq. (1) as a function of  $q$ . The correlation dimension is  $D_2 = 3.1 \pm 0.1$ , see Table 1. The values of  $D_q + 3$  are calculated analytically for the weighted Cantor set with  $p = 0.09$  (dashed-dotted).



the slow solar wind in the inner heliosphere. For comparison, an extremely simple example of the multifractal system is the weighted Cantor set, where the probability of visiting one-third segment is  $p$ , say  $p \leq 1/2$ , and the probability of visiting the removed middle segment is zero, so that the probability of visiting the remaining one-third segment is  $1-p$ . In this case the results can be obtained analytically; for any  $q$  in Eq. (1) one has

$$(1-q)D_q = \log_3[p^q + (1-p)^q]. \quad (4)$$

The difference of the maximum and minimum dimensions associated with the least-dense and most-dense points on the attractor, correspondingly, is  $D_{-\infty} - D_{\infty} = \log_3(1/p-1)$  and in the limit  $p \rightarrow 0$  this difference rises to infinity. Hence, the parameter  $p$  can be regarded as a degree of multifractality. For illustration the results of  $D_q + 3$  calculated for  $p = 0.09$  in Eq. (4) are also shown in Fig. 4 by a dashed-dotted line. We see that the multifractal spectrum of the solar wind is roughly consistent with that for the multifractal measure on the self-similar weighted Cantor set, with a single weighting parameter  $p$ . Admittedly, this is a statistical model with as yet unknown connection with the specific dynamics of the solar wind. The obtained value of the parameter  $p$  merely demonstrates that some cubes that cover the attractor of our dynamical system are visited one order of magnitudes more frequently than some other cubes, as is illustrated in our previous paper, see Fig. 5 of Macek (1998).

Naturally, the value of parameter  $p$  (within the factor of  $\frac{\log 2}{\log 3}$ ) is related to the usual models, which starting from Richardson's version of turbulence, try to recover the observed scaling exponents, which is based on the so-called  $p$ -model of turbulence (e.g., Meneveau and Sreenivasan, 1987). The value of  $p = 0.1$  obtained here is roughly consistent with the fitted value in the literature both for laboratory and the solar wind turbulence, which is in the range  $0.13 \leq p \leq 0.3$  (e.g., Burlaga, 1991; Carbone, 1993; Carbone and Bruno, 1996; Marsch et al., 1996). One should only bear in mind that here we take probability measure directly on the solar wind attractor, which quantifies multifractal nonuniformity of visiting various parts of the attractor in the phase space, while the usual  $p$ -model is related to the solar wind turbulence cascade for the dissipation rate, which resides in the physical space.

We also estimate the Kolmogorov correlation entropy,  $K_2$ , and the largest positive Lyapunov exponent,  $\lambda_{\max}$ . The vertical spacings between the parallel lines in Fig. 2 of (Macek, 2002) averaged in the saturation region  $8 \leq m \leq 10$  are taken as  $K_2$  yielding the value of  $\approx 0.1$  (per delay time  $\tau$ ). Using the algorithm by Kantz (1994) and nonlinear noise reduction, one obtains the magnitude of  $\lambda_{\max} \sim 0.1$  in the same units as for  $K_2$  (base e). In general, the entropy  $K_q$  is at most the sum of the positive Lyapunov exponents  $\sum \lambda_i$  (e.g., Ott,

1993). The value of the Lyapunov exponent is consistent with the Kolmogorov ( $q = 2$ ) entropy, which should be its lower bound:  $K_2 \leq \sum \lambda_i$  (positive). The time over which the meaningful prediction of the behavior of the system is possible is roughly  $\sim 1/\lambda_{\max}$  (e.g., Ott, 1993). Hence the predictability of the system is limited to hours.

The obtained measures of the attractor have been subjected to the surrogate data test (Theiler et al., 1992). As has been demonstrated in Fig. 8 of Macek (1998), if the original data are indeed deterministic, analysis of these surrogate data will provide values that are statistically distinct from those derived for the original data, see also Table 1. In particular, the slope of the correlation sum increases with  $m$  (no saturation), and the Lempel–Ziv complexity calculated for shuffled-data becomes clearly 1.0, as it should be for a purely stochastic system. Again, we have found that the solar wind data are sensitive to this test.

## 5. Conclusions

In conclusion, we have shown that the singular-value decomposition filter removes some amount of noise, which is sufficient to calculate the generalized dimensions of the solar wind attractor. The obtained multifractal spectrum is consistent with that for the multifractal measure on the self-similar weighted Cantor set with a degree of multifractality of  $p \sim 10^{-1}$ . The obtained characteristics of the attractor are significantly different from those of the surrogate data. Thus these results show multifractal structure of the solar wind in the inner heliosphere. Hence we suggest that there exists an inertial manifold for the solar wind, in which the system has *multifractal* structure, and where noise is certainly not dominant. The multifractal structure, convected by the wind, might probably be related to the complex topology shown by the magnetic field at the source regions of the solar wind.

## Acknowledgements

This work has been done in the framework of the European Commission Research Training Network Grant No. HPRN-CT-2001-00314 and has been partially supported by the State Scientific Research Committee (MNI) through Grant No. 2 P03B 126 24.

## References

- Albano, A.M., Muench, J., Schwartz, C., Mees, A.I., Rapp, P.E. Singular-value decomposition and the Grassberger–Procaccia algorithm. *Phys. Rev. A* 38, 3017–3026, 1988.

- Bruno, R., Carbone, V., Veltri, P., Pietropaolo, E., Bavassano, B. Identifying intermittent events in the solar wind. *Planet. Space Sci.* 49, 1201–1210, 2001.
- Burlaga, L.F. Multifractal structure of the interplanetary magnetic field: Voyager 2 observations near 25 AU, 1987–1988. *Geophys. Res. Lett.* 18, 69–72, 1991.
- Burlaga, L.F. Lognormal and multifractal distributions of the heliospheric magnetic field. *J. Geophys. Res.* 106, 15917–15927, 2001.
- Carbone, V. Cascade model for intermittency in fully developed magnetohydrodynamic turbulence. *Phys. Rev. Lett.* 71, 1546–1548, 1993.
- Carbone, V., Bruno, R. Cancellation exponents and multifractal scaling laws in the solar wind magnetohydrodynamic turbulence. *Ann. Geophys.* 14, 777–785, 1996.
- Grassberger, P. Generalized dimensions of strange attractors. *Phys. Lett. A* 97, 227–230, 1983.
- Grassberger, P., Procaccia, I. Measuring the strangeness of strange attractors. *Physica D* 9, 189–208, 1983.
- Halsey, T.C., Jensen, M.H., Kadanoff, L.P., Procaccia, I., Shraiman, B.I. Fractal measures and their singularities: the characterization of strange sets. *Phys. Rev. A* 33, 1141–1151, 1986.
- Hentschel, H.G.E., Procaccia, I. The infinite number of generalized dimensions of fractals and strange attractors. *Physica D* 8, 435–444, 1983.
- Kantz, H. A robust method to estimate the maximal Lyapunov exponent of a time series. *Phys. Lett. A* 185, 77–87, 1994.
- Kaspar, F., Schuster, H.G. Easily calculable measure for the complexity of spatiotemporal patterns. *Phys. Rev. A* 36, 842–848, 1987.
- Kurths, J., Herzog, H. An attractor in a solar time series. *Physica D* 25, 165–172, 1987.
- Macek, W.M. Testing for an attractor in the solar wind flow. *Physica D* 122, 254–264, 1998.
- Macek, W.M. Multifractality and chaos in the solar wind. in: Boccaletti, S., Gluckman, B.J., Kurths, J., Pecora, L.M., Spano, M.L. (Eds.), *Experimental Chaos*, 622. American Institute of Physics, New York, pp. 74–79, 2002.
- Macek, W.M., Obojska, L. Fractal analysis of the solar wind flow in the inner heliosphere. *Chaos, Solitons & Fractals* 8, 1601–1607, 1997.
- Macek, W.M., Obojska, L. Testing for nonlinearity in the solar wind flow. *Chaos, Solitons & Fractals* 9, 221–229, 1998.
- Macek, W.M., Redaelli, S. Estimation of the entropy of the solar wind flow. *Phys. Rev. E* 62, 6496–6504, 2000.
- Mandelbrot, B.B. *Multifractal measures, especially for the geophysicist*. Pure Appl. Geophys., 131. Birkhäuser Verlag, Basel, pp. 5–42, 1989.
- Meneveau, C., Sreenivasan, K.R. Simple multifractal cascade model for fully developed turbulence. *Phys. Rev. Lett.* 59, 1424–1427, 1987.
- Marsch, E., Tu, C.-Y. Non-Gaussian probability distributions of solar wind fluctuations. *Ann. Geophys.* 12, 1127–1138, 1994.
- Marsch, E., Tu, C.-Y. Intermittency, non-Gaussian statistics and fractal scaling of MHD fluctuations in the solar wind. *Nonlinear Proc. Geophys.* 4, 101–124, 1997.
- Marsch, E., Tu, C.-Y., Rosenbauer, H. Multifractal scaling of the kinetic energy flux in solar wind turbulence. *Ann. Geophys.* 14, 259–269, 1996.
- Ott, E. *Chaos in Dynamical Systems*. Cambridge University Press, Cambridge, 1993.
- Schwenn, R. Large-scale structure of the interplanetary medium. in: Schwenn, R., Marsch, E. (Eds.), *Physics of the Inner Heliosphere*, 20. Springer-Verlag, Berlin, pp. 99–182, 1990.
- Theiler, J. Spurious dimension from correlation algorithms applied to limited time-series data. *Phys. Rev. A* 34, 2427–2432, 1986.
- Theiler, J., Eubank, S., Longtin, A., Galdrikian, B., Farmer, J.D. Testing for nonlinearity in time series: the method of surrogate data. *Physica D* 58, 77–94, 1992.